Hindawi
Advances in Materials Science and Engineering
Volume 2019, Article ID 6465196, 9 pages
https://doi.org/10.1155/2019/6465196

Research Article

Springback Study on Profile Flexible 3D Stretch-Bending Process Using the Neural Network

Yi Li,[1,2] **Ce Liang**,[1,2] **Xiangfeng Lin**,[1,3] **Jicai Liang**,[1,3] **Zhongyi Cai**,[1,3] **and Fei Teng**[4]

[1]*Key Laboratory of Automobile Materials (Jilin University), Ministry of Education, Changchun 130025, Jilin, China*
[2]*College of Materials Science and Engineering, Jilin University, Changchun 130025, Jilin, China*
[3]*Roll Forging Institute, Jilin University, Changchun 130025, Jilin, China*
[4]*College of Mechanical and Automotive Engineering, Changchun University, Changchun 130025, Jilin, China*

Correspondence should be addressed to Ce Liang; liangce@jlu.edu.cn

Received 15 June 2019; Accepted 23 September 2019; Published 15 October 2019

Academic Editor: José António Fonseca de Oliveira Correia

The springback is one of the main defects in the flexible 3D stretch-bending process. In this paper, according to the orthogonal design of experiments, the numerical simulation analysis of the springback for the 3D stretch-bending aluminum profile is carried out by the ABAQUS finite element software. And to investigate the effect of material properties on the springback, the range analysis of the orthogonal experiment is performed. The results show that these material properties of the aluminum profile (elastic modulus E, yield strength σ_y, and tangent modulus E_1) might have the biggest influence on the springback of the aluminum profile, and the optimized forming parameters are founded as follows: the horizontal bending degree is 14°, the vertical bending degree is 14°, the number of multipoint stretch-bending dies is 10, the friction coefficient is 0.15, and aluminum alloy grade is 6063. Moreover, the model of the BP neural network for the prediction of the springback is established and trained based on the orthogonal experiment, and the results with the BP neural network model are in good agreement with experimental results. So it is obvious that the BP neural network could predict effectively the springback of 3D multipoint stretch-bending parts.

1. Introduction

In recent years, lightweight requirements have grown more demanding for reduction of energy consumption and environmental pollution caused by exhaust emissions [1–3]; especially, the design of the lightweight part plays a more and more important role in economic and ecological aspects [4]. Aluminum alloy is widely used in aerospace, rail vehicle manufacturing, and automobile manufacturing as a lightweight material because of its low density, high strength, and ease of recycling [5–7].

Aluminum profile can meet many diversified requirements, but the formation of the aluminum profile brings many new problems in the part design and manufacturing process. Because the elastic modulus of the aluminum alloy is only one-third that of the steel sheet, the springback of the aluminum alloy is much bigger than the same data of the steel sheet, and the springback becomes one of the main defects for the aluminum profile stretch-bending part [8]. If not to make reasonable estimation for the springback of the aluminum profile stretch-bending part, it will have serious influence on the forming quality of components and furthermore service life.

There are many influence factors on the springback such as profile characteristics, processing parameters, and die structure. During the flexible 3D multipoint stretch-bending process of the aluminum profile, the springback analysis is very complicated with geometric nonlinearity, material nonlinearity, and contact nonlinearity, so it is hard to find out an accurate mathematical model [9]. The artificial neural network is widely used in the property prediction of the metal material for high ability of nonlinear mapping and prediction of the output target according to the finite training sample [10–12]. Kazan et al. investigated the springback of the metal sheet in the bending process and developed the prediction model for

the springback by using the artificial neural network [13]. Jamli et al. built the springback prediction model for metal sheet stretch bending and L-shaped bending, respectively, based on finite element simulation and artificial neural network [14, 15]. Nasrollahi and Arezoo investigated the springback prediction for a bending area of the metal sheet with hole by the experiment, finite element simulation, and artificial neural network [16]. Babu et al. developed an artificial neural network system to predict the behavior of deep drawing for welding blank made by steel and aluminum alloy [17]. However, the neural network model is not used for the springback prediction of three-dimensional stretched profiles.

Based on the orthogonal experiments, the numerical simulation of the springback in 3D multipoint stretch bending of the aluminum profile is investigated by the ABAQUS finite element software, the training samples of the BP neural network are achieved, and the mapping ability between stretch-bending parameters and output value of the springback is built by using the powerful function mapping ability of the BP neural network. The results show that it can save a lot of simulation time and provide important reference data for the forming precision and springback compensation of the aluminum profile-forming part.

2. Concept and Finite Element Model of Multipoint Stretch Bending (MPSB)

2.1. Principle of the Multipoint Stretch-Bending Process. The multipoint stretch bending (MPSB) is improved on the basis of the traditional stretch bending. The stretch-bending die in the traditional stretch bending is discretized. It can solve the 3D stretch bending of the profiles through the multipoint technology combined with the traditional stretch bending. Therefore, the MPSB process is more diversified than conventional bending process because of the additional vertical bending stage of the profile.

As shown in Figure 1, when the profile is three-dimensionally stretched and formed, the bending machine can move the die units back, forth, up, and down. So the rotation angle of the profile can be adjusted on two planes, thereby decomposing the 3D stretch bending into the horizontal bending and the vertical bending.

2.2. Material Model. Because the aluminum alloys have lightweight and good mechanical properties, they are used widely for structural parts of the railway vehicle. In this study, five aluminum alloy grades are used which are as follows: 6063, 6005A, 5052, 5083, and 6082, the profile length is 3200 mm, and the profile weight is about 3.3 kg. It is assumed that the aluminum material is isotropic, the elastic-plastic constitutive behavior is isotropic hardening, and relevant mechanical properties are as shown in Table 1.

2.3. Setup of Finite Element Model. In the finite element simulation of 3D stretch bending, the reasonable simplification of the finite element model can reduce the calculation time, avoid other problems caused by the complexity of the model, and affect the accuracy of the results. Therefore, it is necessary to rationally simplify the finite element model. As shown in Figure 2, the die is simplified on the stretch-bending machine, using only the die units in contact with the profile, and the limit screw that limits the displacement of the die units in the vertical direction of the x-z plane is simplified as a planar flap, which is 50 mm in length with the die units. Meanwhile, the clamp is simplified to the same shape as the profile and is bound to the profile, the length of which is 100 mm. So only different die sections and clamps need to be replaced when forming different geometric profiles.

When selecting the appropriate element type for the finite element model, not only the accuracy of the simulation result but also the operation time should be considered. It is necessary to obtain the most accurate simulation result in the shortest possible calculation time. The finite element model consists of the aluminum profile, clamp, die units, and limit screw. The unit types and unit and node number information of each component are shown in Table 2.

3. Orthogonal Experiment for the Springback of Aluminum Profile

3.1. Selecting the Level of Various Factors. The orthogonal experiment is a kind of design method which has a good effect to study and deal with multifactor problems, and it is based on the orthogonality of the data to design the scheme. It has the advantage of being able to obtain reliable and representative test results in as few test times as possible. Through the analysis and integration of the test results, the best test conditions can be selected as the optimal level combination of each factor.

In the MPSB process, many factors influence the springback of the aluminum profile such as yield strength, elastic modulus, tangent modulus, bending angle in horizontal and vertical directions, die structure, die clearance, prestretching value, and friction force. According to the stretch-bending process and orthogonal experiment, seven important impact factors are as follows: elastic modulus (E), yield strength (σ_y), tangent modulus (E_1), horizontal bending angle (α), vertical bending angle (β), die number (N), and friction coefficient (μ). Five aluminum alloy grades used in the orthogonal experiment are 6063, 6005A, 5052, 5083, and 6082. The values of each factor level are as shown in Table 3.

3.2. Orthogonal Design. The table of the orthogonal experiment is usually expressed as $L_a(S_1 \times S_2 \times S_3 \times \cdots \times S_b)$, where L is the orthogonal table, a is the test number, b is the maximum value of impact factors, and S_1 - S_b are the value of the impact factor level from column 1 to column 9. The orthogonal experiment can effectively reduce the number of experiments. In this study, the design of the $L_{25}(5^5)$ orthogonal table is selected, and seven impact factors (E, σ_y, E_1, α, β, N, and μ) all select five levels.

The design of the orthogonal experiment and the springback of the aluminum profile are shown in Table 4. And the springback of the aluminum profile is simulated using the ABAQUS software, based on the parameters in the orthogonal

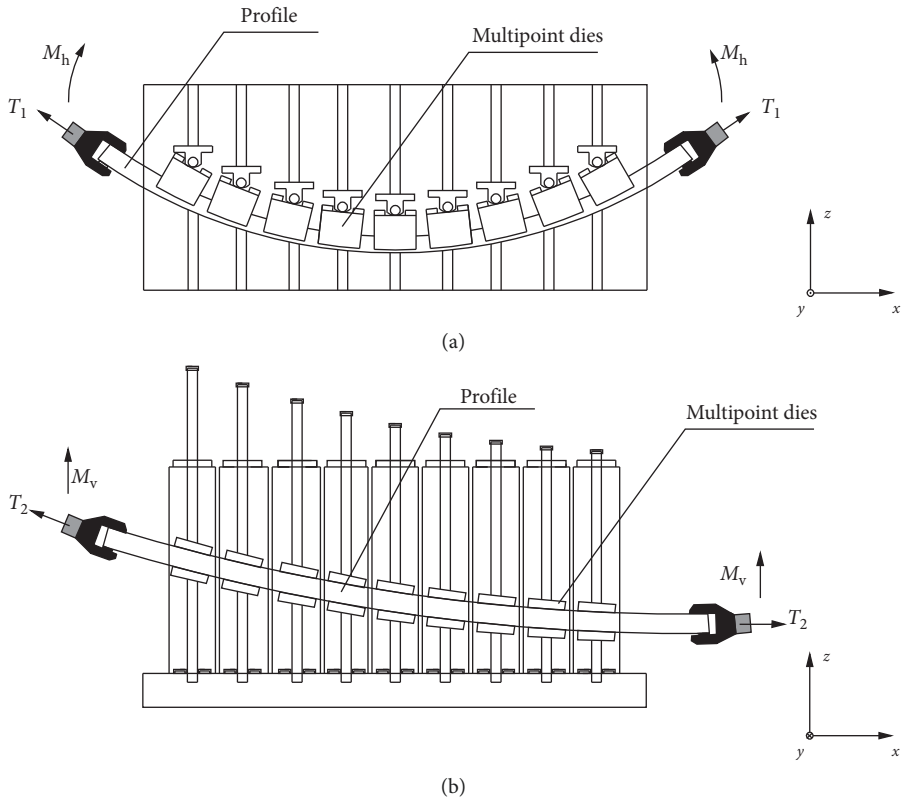

Figure 1: Schematic diagram of the flexible 3D multipoint stretch-bending equipment. (a) Bending forming in the horizontal direction. (b) Bending forming in the vertical direction.

Table 1: Aluminum alloy grade and mechanical properties.

Aluminum alloy grade	Treatment state	Elastic modulus E (MPa)	Tangent modulus E_1 (MPa)	Tensile strength σ_b (MPa)	Yield strength σ_s (MPa)	Poisson's ratio υ	Density ρ (g/cm^3)
6063	T5	68300	341.667	186	145	0.33	2.69
6005A	T5	69000	210	262	241	0.33	2.7
5052	H32	69300	291.667	230	195	0.33	2.68
5083	H112	70300	687.5	303	193	0.33	2.66
6082	T6	71000	666.67	290	250	0.33	2.7

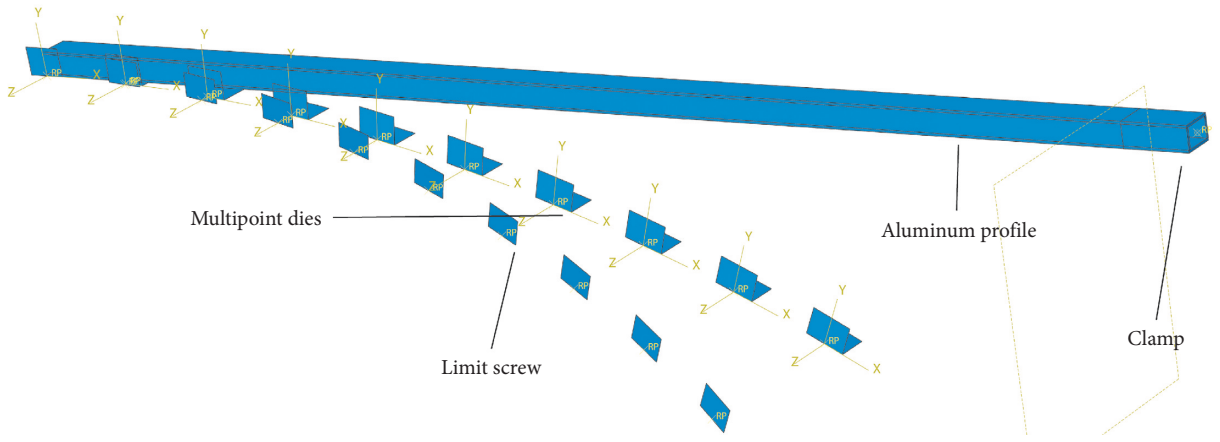

Figure 2: Finite element model for the flexible 3D stretch-bending process.

Table 2: Unit types and number of units and nodes for finite element components.

Finite element components	Unit types	Number of units	Number of nodes
Aluminum profile	C3D8R	9858	13912
Die units	R3D4	216	250
Clamp	R3D4	500	550
Limit screw	R3D4	80	99

Table 3: Levels and impact factors of the orthogonal experiment.

Level	Impact factor				
	A	B	C	D	E
	Alloy grade	α (°)	β (°)	N	μ
1	6063	14	14	4	0.05
2	6005A	18	18	6	0.1
3	5052	22	22	8	0.15
4	5083	26	26	10	0.2
5	6082	30	30	12	0.25

table. In the MPSB process, the aluminum profile is formed along the space curve, which has more complex deformation than the traditional stretch-bending process. So the springback of the 3D stretch-bending process can be divided into two parts, as shown in Figure 3; one part is horizontal springback along the horizontal direction in the x-y plane, and the other part is vertical springback along the vertical direction in the x-z plane. δ_y is the value of horizontal springback in the x-y plane, δ_z is the value of vertical springback in the x-z plane, and δ is the value of total springback for the aluminum profile.

3.3. Range Analysis in Orthogonal Experimental Data. The range analysis table of the orthogonal experiment is shown in Figure 4.

According to Figure 4, the main factors affecting the horizontal springback along the x-y plane in order of importance are elastic modulus (E), yield strength (σ_y), tangent modulus (E_1), friction coefficient (μ), die number (N), horizontal bending angle (α), and vertical bending angle (β). And the main factors affecting the vertical springback along the x-z plane in order of importance are elastic modulus (E), yield strength (σ_y), tangent modulus (E_1), horizontal bending angle (α), die number (N), vertical bending angle (β), and friction coefficient (μ). The main factors affecting the total springback in order of importance are elastic modulus (E), yield strength (σ_y), tangent modulus (E_1), horizontal bending angle (α), die number (N), friction coefficient (μ), and vertical bending angle (β).

3.4. Optimized Parameters and Verification. The optimized parameter combination means that the combination of levels can make test results reach the optimum state in the range of all factors. The optimized parameter combination is founded by the experiment index. The larger the experiment index is, the better the level corresponding to the maximum value of the index selected is. In contrast, the smaller the test index is, the better the level corresponding to the minimum value of the index selected is.

In this study, the experiment index is the value of springback clearance. According to data in Table 5, the best combination for horizontal springback along the x-y plane is $A_4B_1C_5D_1E_3$, and the best combination for vertical springback along the x-z plane and the best combination for total springback are $A_1B_1C_1D_4E_3$. These two combinations have little deviation for horizontal springback along the x-y plane, but the deviation is big for vertical springback along the x-z plane and total springback. So the optimized parameter combination selected in the orthogonal experiment is $A_1B_1C_1D_4E_3$, and the corresponding parameters are as follows: the aluminum alloy material is 6063, horizontal bending angle is 14°, vertical bending angle is 14°, multipoint die number is 10, and friction coefficient is 0.15.

The optimized parameter combination $A_1B_1C_1D_4E_3$ is validated by using the ABAQUS software simulation, and the simulated results are shown in Table 5.

Compared to data in Tables 4 and 5, it is found that the best values of vertical springback and total springback are achieved by using the optimized parameter combination $A_1B_1C_1D_4E_3$, and the deviation is little for horizontal springback. The stress-strain chart of 3D stretch bending under the combination $A_1B_1C_1D_4E_3$ is shown in Figure 5.

As can be seen from Figure 5, the stress and equivalent strain are evenly distributed, and the forming part has no defects. It shows that the forming effect is very good.

4. Prediction of the Springback Based on BP Neural Network

4.1. Setup of BP Neural Network Model. The BP neural network is a kind of multilayer forward feeding neural network. Its main feature is that the signals feed forward and the errors propagate backward. The output error is used to predict the error of the direct leading layer for the output layer. Then, the error of the direct leading layer is used to predict the error of the further layer, and the errors of others layers are gained from layer-by-layer backpropagation [18, 19].

The model of the BP neural network is composed of the input layer, hidden layer, and output layer. The input layer and output layer are usually determined based on the practice problem, the neuron number in the input layer is equal to the dimension of input sample data, and the neuron number in the output layer is equal to the dimension of the result sample. The neuron number in the hidden layer is usually calculated by the following empirical equation [20]:

$$l < \sqrt{m+n} + p, \tag{1}$$

where m is the neuron number in the input layer; n is the neuron number in the output layer; p is the constant, and $1 < p < 10$; and l is the neuron number in the hidden layer.

Table 4: Design and results of the orthogonal experiment.

Number	A	B	C	D	E	Horizontal springback value δ_y (mm)	Vertical springback value δ_z (mm)	Total springback value δ (mm)
1	6063	14	14	4	0.05	2.401	4.673	5.566
2	6063	18	18	6	0.1	3.185	4.711	5.933
3	6063	22	22	8	0.15	2.777	4.953	5.880
4	6063	26	26	10	0.2	3.529	5.289	6.438
5	6063	30	30	12	0.25	3.493	5.918	6.905
6	6005A	14	18	8	0.2	4.133	6.793	8.840
7	6005A	18	22	10	0.25	5.310	7.807	9.955
8	6005A	22	26	12	0.05	5.112	7.345	9.433
9	6005A	26	30	4	0.1	3.166	9.064	9.968
10	6005A	30	14	6	0.15	5.144	8.727	10.41
11	5052	14	22	12	0.1	3.228	5.704	7.033
12	5052	18	26	4	0.15	1.896	6.395	7.118
13	5052	22	30	6	0.2	4.471	7.328	8.626
14	5052	26	14	8	0.25	3.958	5.657	7.211
15	5052	30	18	10	0.05	2.773	5.824	6.818
16	5083	14	26	6	0.25	4.097	6.420	7.864
17	5083	18	30	8	0.05	3.259	7.597	8.324
18	5083	22	14	10	0.1	2.924	5.318	6.718
19	5083	26	18	12	0.15	2.539	6.731	7.628
20	5083	30	22	4	0.2	1.471	6.735	7.791
21	6082	14	30	10	0.15	4.401	6.086	7.500
22	6082	18	14	12	0.2	7.764	7.705	10.94
23	6082	22	18	4	0.25	8.251	9.178	12.30
24	6082	26	22	6	0.05	7.289	9.630	12.09
25	6082	30	26	8	0.1	9.359	9.835	13.70

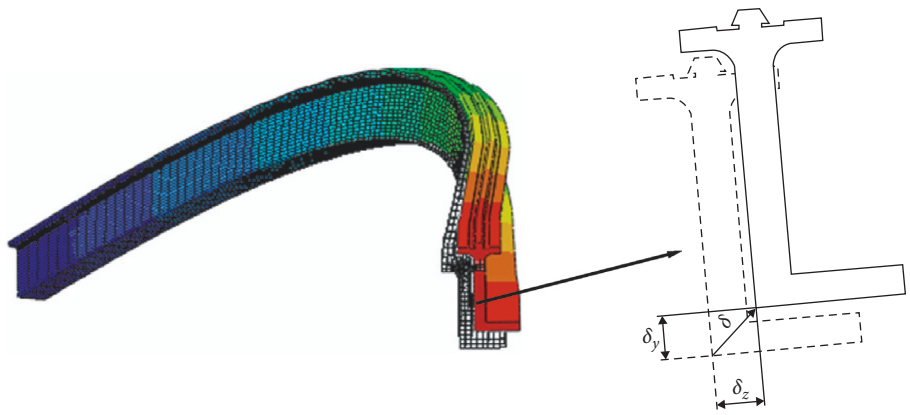

Figure 3: The front and back spatial positions of the end face contours.

In this study, the neuron number in the input layer is 7, and the neuron number in the output layer is 3. The neuron number in the hidden layer is 10 based on the training time and accuracy of the BP neural network. The 7-10-3 three-layer frame of the BP neural network is set up, as shown in Figure 6.

The mathematical model of neural network function which has 10 hidden layers is as follows:

$$y_k = \sum_{j=1}^{10} w_{jk} \times \mathrm{sig}\left(\sum_{i=1}^{7} w_{ij} \times x_i + b_j\right) + b_k \quad (k = 1, 2, 3), \tag{2}$$

where w_{ij} is the weight of the input layer to the hidden layer, w_{jk} is the weight of the hidden layer to the output layer, b_j is the offset weight of the hidden layer, b_k is the offset weight of the output layer, sig is the sigmoid activation function, x_i is the input value of the neural network, and y_k is the output value of the neural network.

4.2. Training and Testing of BP Neural Network. The data are normalized before training the BP neural network in order to avoid large difference order of magnitude of the input-output data result in big error of prediction, and the

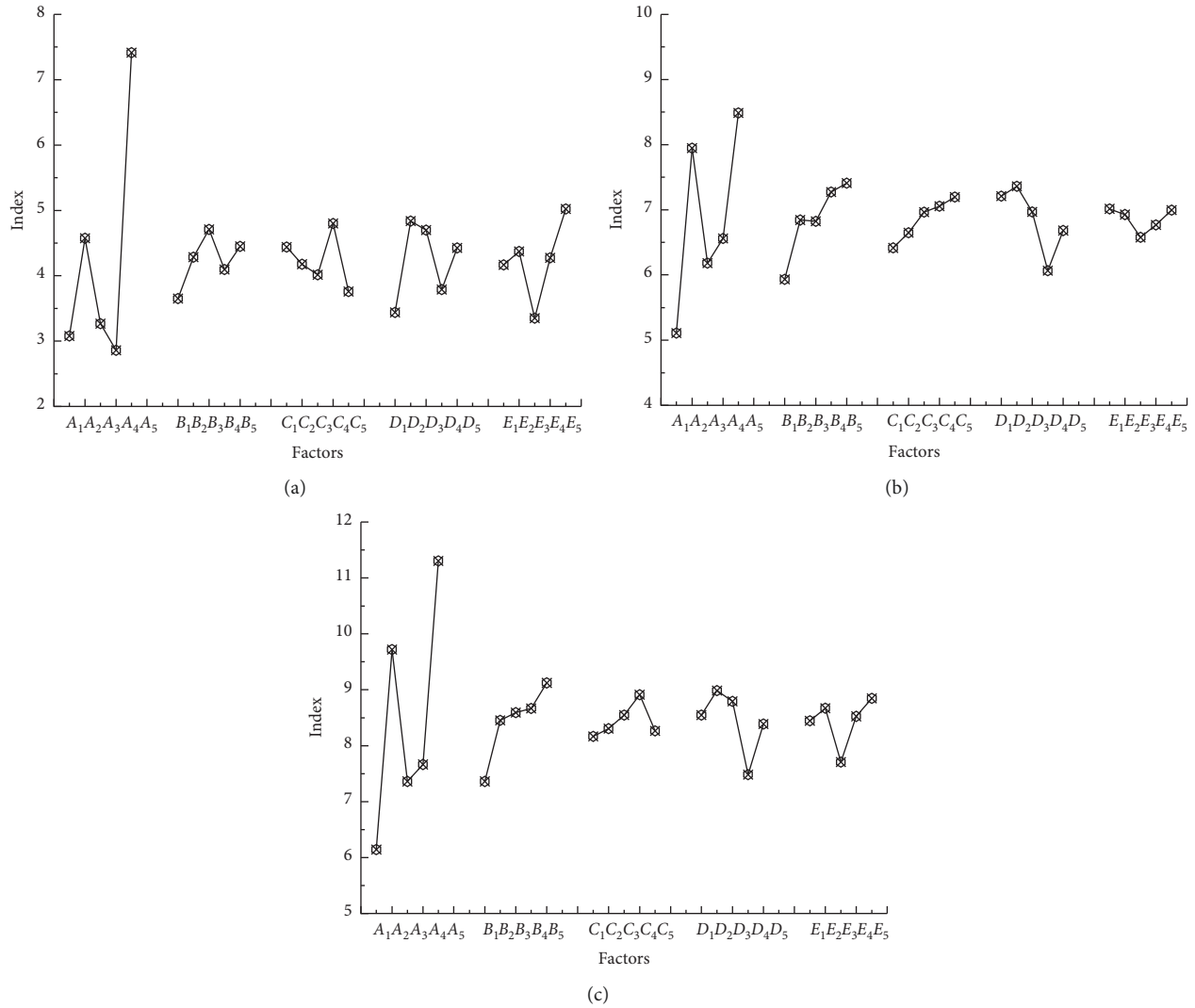

Figure 4: Relationship between experimental factors and springback index: (a) horizontal springback; (b) vertical springback; (c) total springback.

Table 5: Springback value of the optimized parameter combination.

Optimized parameter combination	δ_y (mm)	δ_z (mm)	δ (mm)
$A_1B_1C_1D_4E_3$	2.354	4.098	5.204

maximum-minimum method is applied on the normalization of data:

$$x_k' = 2 \times \frac{x_k - x_{\min}}{x_{\max} - x_{\min}} - 1, \quad (3)$$

where x_k' is the value after the normalization of the data sequence, $x_{\max}$ is the maximum value of the data sequence, and $x_{\min}$ is the minimum value of the data sequence.

The training parameters are as follows: the maximum training time is 10000, the expected training error is $1e^{-6}$, the learning rate is 0.02, and the momentum factor is 0.65. A total of 41 pairs of data in which 15 pairs of simulated data are from ABAQUS software are used for training and testing the BP neural network. Among these data, under the optimized parameter combination $A_4B_1C_5D_1E_3$, orthogonal experiment sample nos. 7, 13, 19, and 25 are used for sample testing, and the others are used for training the BP neural network. The comparison of finite element simulation and prediction results of the BP neural network after MATLAB training is shown in Figure 7.

As seen from Figure 7, it is shown that there is little difference between the prediction results of the BP neural network and the simulation results, the training accuracy is high, so the BP neural network method can replace the finite element simulation to predict the springback of the 3D stretch-bending process, reduce the simulation runtime, and increase the simulation efficiency.

4.3. Test Verification. To validate the finite element simulation and BP neural network on the springback of the 3D

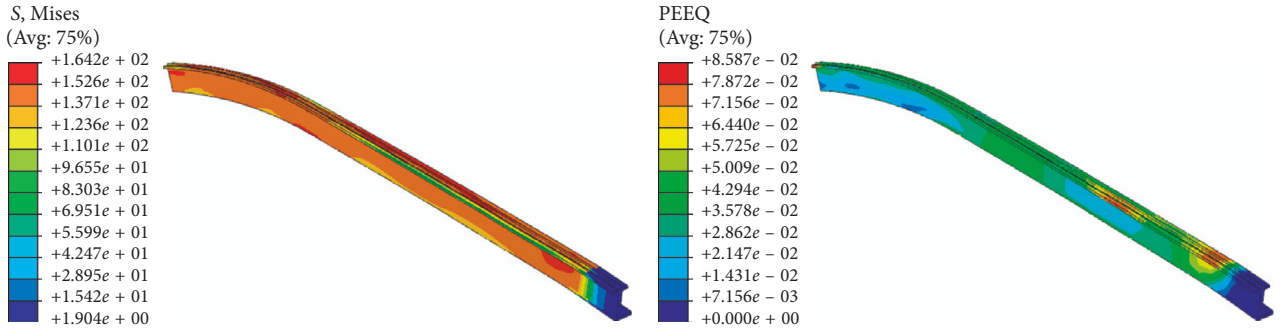

(a) (b)

Figure 5: Stress-strain chart of 3D stretch bending (combination $A_1B_1C_1D_4E_3$).

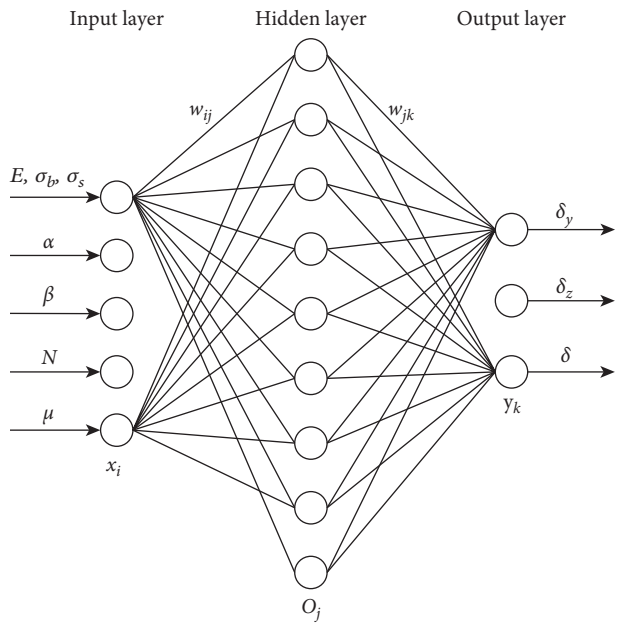

Figure 6: Frame chart of the BP neural network.

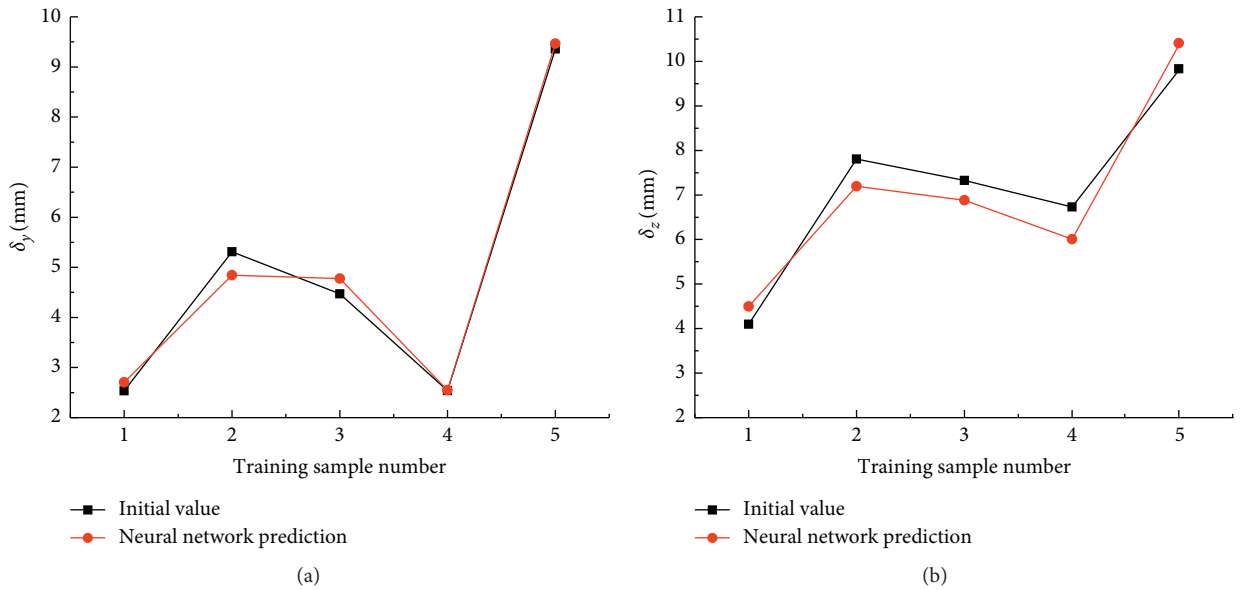

(a) (b)

Figure 7: Continued.

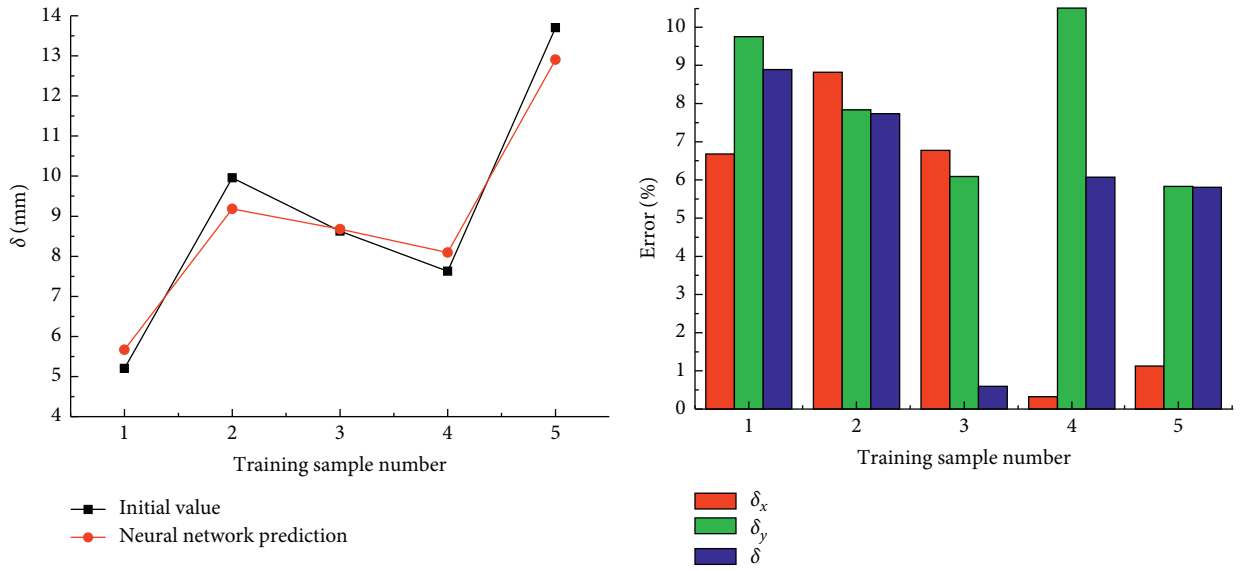

(c) (d)

Figure 7: Stress-strain chart of 3D stretch bending (combination $A_1B_1C_1D_4E_3$).

Figure 8: The detection setup and the forming part through the MPSB process.

Table 6: Comparison of experimental results, simulation results, and BP neural network-predicted results.

	Horizontal springback value δ_y (mm)	Vertical springback value δ_z (mm)	Total springback value δ (mm)
Experimental results	2.79	4.55	5.73
Simulation results	2.53	4.10	5.20
BP neural network-predicted results	2.70	4.50	5.67

stretch-bending process, the comparison of experimental results, simulation results, and prediction results is investigated. The experimental results are founded based on the optimized parameter combination $A_1B_1C_1D_4E_3$, whose forming parameters are as follows: the aluminum alloy material is 6063, horizontal bending angle is 14°, vertical bending angle is 14°, multipoint die unit number is 10, and friction coefficient is 0.15. The detection setup and the forming part through the MPSB process are shown in Figure 8.

The detection setup is used to detect the value of the springback after stretch bending of the aluminum profile, as shown in Figure 8, and the detected values are shown in Table 6.

As seen from Table 6, the results with the BP neural network model and simulation results are in good agreement with experimental results. Therefore, it is obvious that a new prediction method of the springback in the flexible 3D stretch-bending process is provided by using the BP neural network.

5. Conclusion

(1) According to the range analysis of the orthogonal experiment, the main factors affecting the springback in the 3D stretch-bending process in order of importance are elastic modulus (E), yield strength (σ_y), and tangent modulus (E_1), and it is shown that the material properties of the aluminum profile should be considered firstly; then, the forming parameters of the 3D stretch-bending process are investigated.

(2) Based on the orthogonal experiment and the influence on the springback, the optimized parameter combination is as follows: the aluminum alloy material is 6063, horizontal bending angle is 14°, vertical bending angle is 14°, multipoint die number is 10, and friction coefficient is 0.15.

(3) Compared to orthogonal experimental data, the results of BP neural network simulation show that it is an effective way to predict the springback by using the BP neural network and provide a new method for practice production.

Data Availability

The data used to support the findings of this study are available from the corresponding author upon request.

Conflicts of Interest

The authors declare that there are no conflicts of interest regarding the publication of this paper.

Acknowledgments

This work was supported by the National Natural Science Foundation of China (51675225).

References

[1] D.-S. Shim, G.-Y. Baek, G.-Y. Shin, H.-S. Yoon, K.-Y. Lee, and K.-H. Kim, "Investigation of tension force in stretch forming of doubly curved aluminum alloy (Al5083) sheet," *International Journal of Precision Engineering and Manufacturing*, vol. 17, no. 4, pp. 433–444, 2016.

[2] T. Liu, Y. Wang, J. Wu et al., "Springback analysis of Z & T-section 2196-T8511 and 2099-T83 Al-Li alloys extrusions in displacement controlled cold stretch bending," *Journal of Materials Processing Technology*, vol. 225, pp. 295–309, 2015.

[3] J. Liang, S. Gao, F. Teng, P.-Z. Yu, and X.-J. Song, "Flexible 3D stretch-bending technology for aluminum profile," *The International Journal of Advanced Manufacturing Technology*, vol. 71, no. 9–12, pp. 1939–1947, 2014.

[4] Y. Zhou, P. Li, M. Li, and L. Wang, "Application and correction of L-shaped thin-wall aluminum in flexible-bending processing," *The International Journal of Advanced Manufacturing Technology*, vol. 92, no. 1–4, pp. 981–988, 2017.

[5] S. Chatti, M. Hermes, A. E. Tekkaya, and M. Kleiner, "The new TSS bending process: 3D bending of profiles with arbitrary cross-sections," *CIRP Annals*, vol. 59, no. 1, pp. 315–318, 2010.

[6] H. Zhu and K. A. Stelson, "Modeling and closed-loop control of stretch bending of aluminum rectangular tubes," *Journal of Manufacturing Science and Engineering*, vol. 125, no. 1, pp. 113–119, 2003.

[7] C.-L. Yu and X.-Q. Li, "Theoretical analysis on springback of L-section extrusion in rotary stretch bending process," *Transactions of Nonferrous Metals Society of China*, vol. 21, no. 12, pp. 2705–2710, 2011.

[8] R. Lu, X. Liu, Z. Xu, X. Hu, Y. Shao, and L. Liu, "Simulation of springback variation in the U-bending of tailor rolled blanks," *Journal of the Brazilian Society of Mechanical Sciences and Engineering*, vol. 39, no. 11, pp. 4633–4647, 2017.

[9] X. Lin, Y. Li, Z. Cai et al., "Effect of flexible 3D multipoint stretch bending dies on the shape accuracy and the optimal design," *Advances in Materials Science and Engineering*, vol. 2018, Article ID 1095398, 9 pages, 2018.

[10] F. Han, J.-H. Mo, H.-W. Qi, R.-F. Long, X.-H. Cui, and Z.-W. Li, "Springback prediction for incremental sheet forming based on FEM-PSONN technology," *Transactions of Nonferrous Metals Society of China*, vol. 23, no. 4, pp. 1061–1071, 2013.

[11] Y. Song and Z. Yu, "Springback prediction in T-section beam bending process using neural networks and finite element method," *Archives of Civil and Mechanical Engineering*, vol. 13, no. 2, pp. 229–241, 2013.

[12] H. Aguir, H. BelHadjSalah, and R. Hambli, "Parameter identification of an elasto-plastic behaviour using artificial neural networks-genetic algorithm method," *Materials & Design*, vol. 32, no. 1, pp. 48–53, 2011.

[13] R. Kazan, M. Fırat, and A. E. Tiryaki, "Prediction of springback in wipe-bending process of sheet metal using neural network," *Materials & Design*, vol. 30, no. 2, pp. 418–423, 2009.

[14] M. R. Jamli, A. K. Ariffin, and D. A. Wahab, "Integration of feedforward neural network and finite element in the draw-bend springback prediction," *Expert Systems with Applications*, vol. 41, no. 8, pp. 3662–3670, 2014.

[15] M. R. Jamli, A. K. Ariffin, and D. A. Wahab, "Incorporating feedforward neural network within finite element analysis for L-bending springback prediction," *Expert Systems with Applications*, vol. 42, no. 5, pp. 2604–2614, 2015.

[16] V. Nasrollahi and B. Arezoo, "Prediction of springback in sheet metal components with holes on the bending area, using experiments, finite element and neural networks," *Materials & Design (1980–2015)*, vol. 36, pp. 331–336, 2012.

[17] K. V. Babu, R. G. Narayanan, and G. S. Kumar, "An expert system for predicting the deep drawing behavior of tailor welded blanks," *Expert Systems with Applications*, vol. 37, no. 12, pp. 7802–7812, 2010.

[18] H.-Y. Li and X.-C. Lu, "Springback and tensile strength of 2A97 aluminum alloy during age forming," *Transactions of Nonferrous Metals Society of China*, vol. 25, no. 4, pp. 1043–1049, 2015.

[19] Z. Fu and J. Mo, "Springback prediction of high-strength sheet metal under air bending forming and tool design based on GA–BPNN," *The International Journal of Advanced Manufacturing Technology*, vol. 53, no. 5–8, pp. 473–483, 2011.

[20] X. Wang and F. Shi, *Analysis of 43 Cases of MATLAB Neural Network*, Beihang University Press, Beijing, China, 2013.